Sensors and Actuators B 195 (2014) 324–331

Contents lists available at ScienceDirect

Sensors and Actuators B: Chemical

journal homepage: www.elsevier.com/locate/snb

Relevance of radiative transfer processes on Nd^{3+} doped phosphate glasses for temperature sensing by means of the fluorescence intensity ratio technique

C. Pérez-Rodríguez [a,*], L.L. Martín [a], S.F. León-Luis [a,b], I.R. Martín [a,b], K. Kiran Kumar [c], C.K. Jayasankar [c]

[a] Departamento de Física Fundamental y Experimental, Electrónica y Sistemas, Universidad de La Laguna, Av. Astrofísico Francisco Sánchez, s/n, E-38206 La Laguna, Tenerife, Spain
[b] MALTA Consolider Team, Instituto de Materiales y Nanotecnología (IMN), Universidad de La Laguna, Av. Astrofísico Francisco Sánchez, s/n, E-38206 La Laguna, Tenerife, Spain
[c] Department of Physics, SriVenkateswara University, Tirupati 517502, India

ARTICLE INFO

Article history:
Received 5 April 2013
Received in revised form
24 November 2013
Accepted 9 January 2014
Available online 25 January 2014

Keywords:
Optical temperature sensor
Nd^{3+}
Energy transfer
Fluorescence Intensity Ratio
Thermal sensitivity
Phosphate glasses

PACS:
78.20.N– Thermo–optic effects
78.55.–m Photoluminescence
Properties and materials

ABSTRACT

We analyze the suitability of Nd^{3+} doped phosphate glasses as optical temperature sensors based on the response of their luminescence bands to temperature. At room temperature, laser excitation of the sample at 532 nm results in an emission spectrum with an intense band centered at 880 nm and an adjacent weak broad band centered at 810 nm, corresponding to the Nd^{3+} ion transitions: $^4F_{3/2} \rightarrow {}^4I_{9/2}$ and $^4F_{5/2} \rightarrow {}^4I_{9/2}$ respectively. Because of thermalization effects between the next $^4F_{3/2}$ and $^4F_{5/2}$ energy levels ($\Delta E \approx 908\,cm^{-1}$), a detectable change on the relative intensities of these emission bands occurs when temperature is increased, affording the experimental calibration of the fluorescence intensity ratio with temperature in the range 300–850 K. It has been shown that the radiative transfer processes favored by the content of Nd^{3+} ions are also responsible for changes to the spectra shapes and so play an important role in the fluorescence intensity ratio. A reliable thermal sensing operation was obtained in a 0.1 mol% doped Nd^{3+} phosphate glass with relative sensitivity values ranging from $153 \times 10^{-4}\,K^{-1}$ at 300 K to $22 \times 10^{-4}\,K^{-1}$ for 850 K, demonstrating good prospects for optical temperature measurements compared to other reported results. However, the reabsorption measurements seen in the samples with a higher Nd^{3+} content reveal that the reliability of the sensing performance is compromised with the doping concentration and the experimental conditions of the measurement.

© 2014 Elsevier B.V. All rights reserved.

1. Introduction

Of note among the various optical methods for developing temperature sensors are those based on luminescence properties [1,2]. These sensors analyze the thermally induced changes in the spectral features of the light emitted by ions, such as intensity, phase, polarization, wavelength, lifetime and band shape. Therefore spectral analysis is required to obtain temperature information with these sensors. These kinds of systems demonstrate advantages over their electrical counterparts as they are free from electromagnetic interference, are electrically isolated, show a wide dynamic range and can sense the emission remotely through a transparent medium without the need for wires or coupling devices [3]. Regarding their construction and the region measured, these systems are designed to be small sized [4,5] or distributed [3]. As with several other sensing devices, temperature optical sensors are widely proposed in the form of optical fibers since, apart from their inherent light guiding of the luminescence, this construction also confers light weight, small size and low cost [6]. Linked with the optical fibers, the trivalent Rare Earth (RE) elements have been one the most reported luminescence centers in the literature. Several fluorescence emissions from RE^{3+} in adequate hosts have exhibited spectral changes associated with a temperature variation. Some remarkable examples are the variations in the intensity of the emission lines from Eu^{3+} in La_2O_2S [7], or the thermal induced evolution of the Ce^{3+} emission decays in YAG nanocrystals [8].

Uniquely, the RE^{3+} luminescence emitters - Pr^{3+}, Nd^{3+}, Sm^{3+}, Ho $^{3+}$, Er^{3+}, Dy^{3+}, Er^{3+} and Yb^{3+} - undergo modifications in the

* Corresponding author. Tel.: +34922318651.
E-mail addresses: cjperez@ull.es, cjpr86@gmail.com (C. Pérez-Rodríguez).

http://dx.doi.org/10.1016/j.snb.2014.01.037
0925-4005/© 2014 Elsevier B.V. All rights reserved.

band shapes of specific emissions due to the effect of the temperature that suggest its study for sensing applications. The band shape change is caused by a thermally induced population redistribution between two adjacent energy levels of the emitting center. In the aforementioned ions there is a high probability of non-radiative transitions between the two energy levels that causes them to be thermally coupled states, additionally, each level is optically coupled to a lower common level [9]. Hence, the intensities associated with the relaxations from the thermalized pairs are temperature dependent, as is the ratio between these intensities, which would be the measurable output of the sensor. The advantages of this measurement, known as the Fluorescence Intensity Ratio (FIR) method, are that it reduces the influences of different factors such as measuring conditions, resolution and time exposures [10]. The relative intensities of the luminescence bands should depend only on temperature and not on the local concentration of the emitting center.

However, these luminescence systems may present some difficulties caused by the superposition of different effects that influence the unambiguous interpretation of the signals. One example is the Eu^{3+} ion, in which the thermal response of its FIR varies by almost an order of magnitude when the temperature is increased only a few tens of degrees. This behavior points to a potential emitter with an excellent sensitivity; unfortunately, the FIR method as applied to Eu^{3+} is not reliable because this hyperthermal sensitivity has been shown to rely on the strong thermal dependence of its energy transfer rate [11–13] and not on the thermal coupling of the levels. This fact exemplifies that several aspects related to the origin of the luminescence at the microscopic level must be considered in order to obtain an optimized optical temperature sensor based on the RE^{3+} luminescence features. In general terms, the key factors are the properties of the host, the choice of RE^{3+} ions, the concentration in which they are found and the transitions considered.

Our aim in this work is to fully characterize the luminescence of Nd^{3+} doped phosphate bulk glasses with different doping concentrations so as to gain an insight into its application to thermometry. The phosphate matrix possesses the suitable qualities for optical sensors provided in Wade's conscientious thesis [6], since it provides a favorable environment for the intense emission of the Nd^{3+} doping ions [14,15]. As demonstrated in this work, they have a wide thermal operating range between 300–850 K and can be manufactured in the form of optical fibers with good mechanical properties [16]. They also have a low manufacturing cost [17]. Contrary to the continuous attention aroused by Er^{3+} doped materials [5,18–21], the FIR thermal response of Nd^{3+} was the object of only a few reports in the early 2000' [6,22]. However, since very recently it has started to attract attention and this use of the ion has been reported in a variety of forms: bulk, microspheres and nanoparticles [4,10,23]. There are several reasons that support this interest. First, for thermal sensing purposes, the Nd^{3+} ion exhibits several luminescence transitions from the thermally coupled energy levels $^4F_{5/2}$ and $^4F_{3/2}$ that are attainable under excitation with low-cost, diode-pumped, solid-state lasers. Among these possible transitions, the relaxations $^4F_{3/2} \rightarrow {}^4I_{9/2}$ (890 nm) and $^4F_{5/2} \rightarrow {}^4I_{9/2}$ (810 nm) yield a sensitivity value in FIR that is higher compared to those terminating at the $^4F_{11/2}$ or $^4F_{13/2}$ levels [6]. The spectral shape of the former transitions shows well separated bands without overlaps, which is critical to reducing errors when determining the fluorescence intensity ratio. Moreover, the 800 and 890 nm emissions lying in the operating range of inexpensive CCD detectors is a feature that enables its industrial production. For these reasons, we can conclude that the promising results of the Nd^{3+} fluorescence intensity ratio response are associated with the relaxations $^4F_{3/2} \rightarrow {}^4I_{9/2}$ and $^4F_{5/2} \rightarrow {}^4I_{9/2}$, and hence these are the transitions studied in this work in keeping with the example in most of the available FIR reports involving Nd^{3+}. In addition, the energy level distribution of the Nd^{3+} ion permits employing an indirect pumping at 532 nm to populate the $^4F_{3/2}$ level that is well separated from the spectral emissions being analyzed. This strategy is used here in order to avoid the errors caused by detecting the laser overlapped with the emission bands, and is suggested since it simplifies the detection of fluorescence. We note here that the prototype shown in reference [6] exemplifies temperature measurement without the need for either spectrographs or optical spectrum analyzers. It uses a simple scheme consisting mainly of an Nd^{3+} doped silica fiber as sensing material coupled by a fiber coupler arrangement to low-cost excitation and detection branches, consisting respectively of an 808 nm laser diode and two silicon detectors with proper band pass filters for each of the aforementioned transitions. The output of the silicon detectors is just measured with voltmeters, and the proper ratio of these measurements is proportional to FIR and related to the temperature of the doped fiber surroundings. The fact that FIR thermal sensing is not constrained to bulk shapes makes it possible to apply this method to biomedicine. U. Rocha et al. [23] propose a scheme in which a solution of Nd^{3+} doped LaF_3 nanoparticles can sense temperature variations in the biological range for human tissues, and indicate its potential use as tool for early disease detection and control of thermal treatments.

These sensor applications require high fluorescence intensities to yield a good signal to noise ratio when using low-cost detectors. Since the power of the pumping laser should be low to avoid optically heating the glass, the dopant concentration is the parameter to optimize in order to obtain a bright emission. Recent results [24] show that certain concentrations of Er^{3+} in fluorotellurite bulk glasses cause the FIR response to be dependent on the zone in the sample where the spectra are measured due to reabsorption effects. Reabsorption, due to the overlap between the absorption and emission spectra, is for most luminescence applications an important loss factor to be avoided. Regarding the FIR application, this effect can be a source of disagreement with the theory according to reference [24]. To investigate the relevance of this effect in the Nd^{3+} doped phosphate glass under study, we tested the FIR in a set of samples with different concentrations of dopants. A. Stoita et al. proposed in [25] an experimental arrangement useful for determining the reabsorption effects on the luminescence lifetimes and that is used extensively here for measuring emission spectra. The work by Stoita et al. reveals that the reabsorption and total internal reflection effects can significantly affect the result of the lifetime measurements if certain experimental conditions are not established. Taking these results into account we have researched the correlation between the FIR response and the concentration of Nd^{3+} in phosphate glasses.

2. Experimental methods

This section describes the experimental procedure, from sample preparation to optical measurements, followed to obtain the information presented in this paper.

2.1. Glass preparation

A conventional melt-quenching method was used to fabricate the phosphate glasses doped with Nd^{3+}. The glasses presented in this study have the following chemical compositions: $(59-x/2)$ P_2O_5, 17.45 K_2O, 14.55 BaO, 9 Al_2O_3 and xNd_2O_3 with $x = 0.1$, 2 or 4. They are labeled PKBANx. To ensure a very smooth surface the glass samples were carefully polished with a carbide abrasive paper and then with a FIS polishing film. Their resulting thickness was 0.8 mm. Specimens in the shape of 1 cm squares were extracted from the preliminary samples by means of a diamond point cutter. A refractive index of 1.525 was measured on an Abbe refractometer

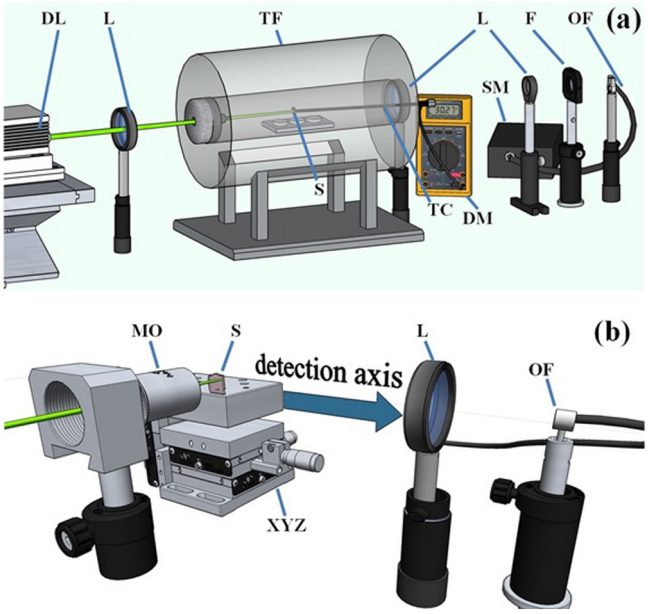

Fig. 1. Experimental set-ups employed for the (a) temperature emission spectra calibration and (b) determination of the reabsorption inside the sample. The correspondence between the acronym labels and the elements in the set-ups is as follows: (a) DL Diode Laser, L Lens, TF Tubular Furnace, S Sample, F Filter, OF Optical Fiber. TC Thermocouple, DM Digital Multimeter, SM Spectrophotometer, additionally in (b): MO Microscope Objective, XYZ translation stage. (Note that the furnace has been depicted with transparency in order to enable the appreciation of the elements).

at sodium wavelength (589.3 nm) with 1-bromonapthalene as the contact liquid.

2.2. Absorption spectra

The optical absorption spectra of the glass samples in the range from 700 to 950 nm were measured with a PerkinElmer Lambda 9 spectrophotometer at room temperature.

2.3. Thermal spectra response

For the luminescence temperature dependence study, each sample was placed inside a horizontal tubular furnace in which a heating rate of 1 K/min was applied. The excitation and luminescence detection branches were aligned along the axis of the furnace as shown in the diagram in Fig. 1(a). On one side of the furnace a 532 nm Nd-YAG laser was focused by a lens on the bulk sample, while on the other side a system of two lenses collimated and focused the emission at the tip of an optical fiber. A high pass filter was placed in the path of the emission collection branch in order to filter the excitation beam. The luminescence spectra were recorded using a CCD Spectrophotometer (Ocean Optics HR4000, resolution 1 nm) coupled to the optical fiber (Thorlabs M25L02, spectral range: 400 to 2400 nm, core diameter 200 μm, NA 0.22). The temperature was monitored with a K-type thermocouple connected to a digital multimeter and situated very close to the sample without touching it. The temperature range analyzed was from room temperature to 850 K. Both sides of the furnace were thermally isolated from the outside, the excitation side by a mullite cover with a small hole in the center that allowed the excitation beam to pass, while the detection side was nearly completely covered by the collimating lens. The power of the excitation laser was checked to be low enough in order to avoid laser heating of the sample. This experimental setup is commonly employed to measure the thermal dependences of spectra, as described in refs [3,10,26,27]. Because of the placement of the sample inside the tubular furnace, no special care could be taken on choosing the bulk sample region from which the collected light spectra were measured.

2.4. Reabsorption measurements

These measurements were performed in order to study the influence on the spectral shape of increasing the emission optical path through the glass. The set-up was configured so as to have a 90° angle between the excitation and detection axes with the sample placed on a translation stage that allowed it to be moved along the axis of the detection branch. A diagram of this set-up is given in Fig. 1(b), where a blue arrow is used to show the direction and orientation of the sample translation. The sample was oriented with the narrower side facing the detector and the wider side facing the excitation. A 20× microscope objective lens (Mitutoyo, M-Plan NIR, NA = 0.4) was employed to focus the 532 nm excitation beam at points located on the wider face of the sample as the translation stage was moved. The detection branch consisted of a 60 mm convergent lens that focused the emission at the tip of an optical fiber (Thorlabs M25L02, spectral range: 400 to 2400 nm, core diameter 200 μm, NA 0.22) coupled to an Andor CCD spectrophotometer with a 0.3 nm spectral resolution. To compare the spectra measured by two different sets of detector equipment, both data were corrected for instrument response.

3. Theoretical background

3.1. Fluorescence intensity ratio technique

Fluorescence intensity ratio is a kind of temperature determination technique based on the change in the band shape luminescence, generally from a RE doped material. The technique studies the relative intensities of two radiative transitions, one between the electronic energy levels E_2 and E_1 and the other from the upper energy level E_3 to E_1, as shown in the left labels of the energy levels in Fig. 2(a). The proximity between the electronic levels E_2 and E_3 allows the upper level to be populated from the E_2 population by thermal redistribution. Thus, the intensity ratios of these transitions depend on the temperature, but they are independent of the source power intensity since the population of each level it is also proportional to the pump power employed. Under low pump power excitation the relative population between the two emitting levels, R, follows a Boltzmann-type population distribution given by [3]:

$$R = \frac{I_{31}}{I_{21}} = \frac{c_3(\nu)\beta_{31}A_3g_3h\nu_3}{c_2(\nu)\beta_{21}A_2g_3h\nu_2}\exp\left(-\frac{E_{32}}{K_BT}\right) = B\exp\left(-\frac{E_{32}}{K_BT}\right) \text{ with } B = \frac{c_3(\nu)\beta_{31}A_3g_3h\nu_3}{c_2(\nu)\beta_{21}A_2g_3h\nu_2} \quad (1)$$

where K_B is the Boltzmann constant, E_{32} is the energy gap between the two excited levels E_3 and E_2, $h\nu_i$ is the average photon energy of each band, g_i is the degeneracy *(2J +1)* of the *i*th level, A_3 and A_2 are the spontaneous radiative rates of the E_3 and E_2 levels, respectively, β_{31} and β_{21} represent the branching ratio of the transitions with respect to ground state and T is the absolute temperature. The $c_i(\nu)$ in this equation has to do with the instrument response. Since the emission spectra have been corrected for the instrument response, this coefficient can be assumed to be unity. The I_{31} and I_{21} correspond to the intensity of the luminescence associated with the transitions to E_1 from states E_3 and E_2 respectively. In this work these emission intensities have been determined by integrating each transition band over the proper wavelength range, with the limits defined by the shape of the band. These limits correspond to 780–845 nm for the transition band associated with $^4F_{5/2} \rightarrow {}^4I_{9/2}$ and 845–925 nm for the $^4F_{3/2} \rightarrow {}^4I_{9/2}$ transition. These ranges

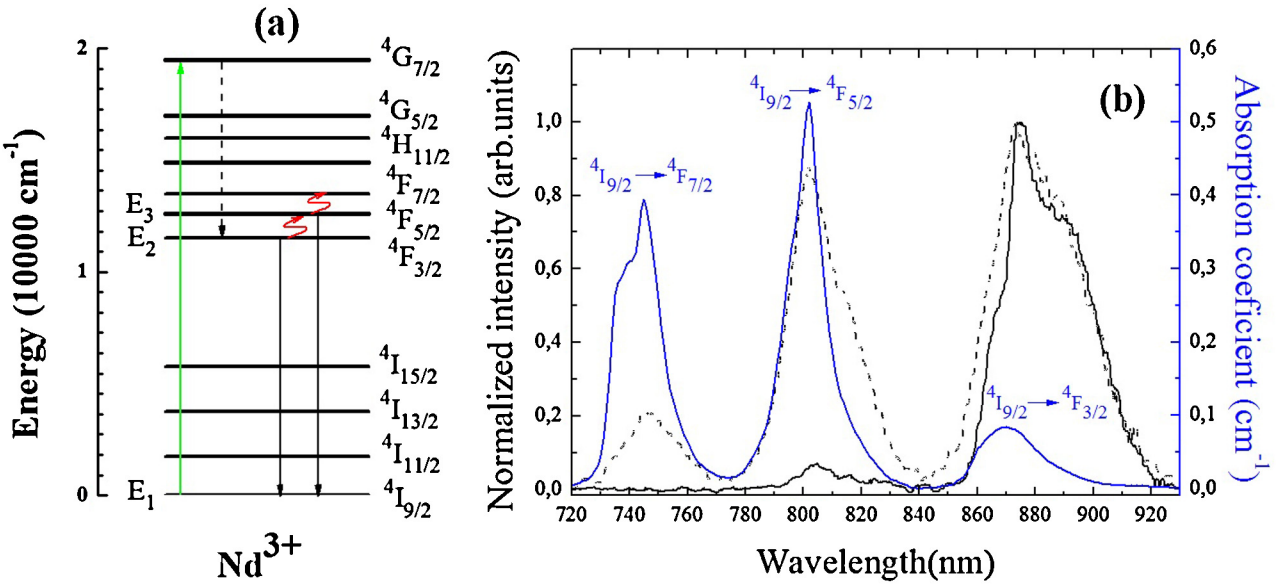

Fig. 2. (a) Partial energy levels diagramof the Nd^{3+} ions showing the 532 nm pumping and the transitions that originate the 880 nm and the 810 nm emissions. (b) Room temperature absorption spectrum and emission spectra at 310 K and 693 K obtained in a PKBAN glass doped with 0.1 mol % Nd^{3+}. The absorption coefficient is plotted in blue continuous line and the emission spectra obtained after 532 nm excitation are plotted in black continuous line for 310 K and in black dashed line for 693 K. (For interpretation of the references to colour in this figure legend, the reader is referred to the web version of this article.).

determine the Boltzmann fitting and therefore establish the application of the temperature calibration. The energy levels of the Nd^{3+} emitters in the phosphate glass samples studied are shown partially in Fig. 2(a). In this ion the FIR involves the levels E_3: $^4F_{5/2}$, E_2: $^4F_{3/2}$ and E_1: $^4I_{9/2}$, with the corresponding transitions being $^4F_{5/2} \rightarrow {}^4I_{9/2}$ and $^4F_{3/2} \rightarrow {}^4I_{9/2}$.

All the pre-exponential factors can be grouped together in the B factor, which is determined using the Judd-Ofelt theory to calculate the rates A_3, A_2 and the branching ratios β_{31} and β_{21}. The Judd-Ofelt parameters of the PKBAN Nd^{3+} doped glass samples were determined in the review of [14] and resulted in $\Omega_2 = 9.23 \times \cdot 10^{-20}\,cm^2$, $\Omega_4 = 7 \times 10^{-20}\,cm^2$ and $\Omega_6 = 8.74 \times 10^{-20}\,cm^2$. Using the value of $E_{32} = 908\,cm^{-1}$ from the absorption spectrum, the theoretical FIR dependence R_{th} yields:

$$R_{th} = 5.36 \exp\left(-\frac{908}{K_B T}\right) \quad (2)$$

3.2. Sensitivity

A key descriptive parameter of a sensor is its sensitivity S, which gives an estimate of how the sensor output reacts when the value of the measured quantity changes. For a fluorescence intensity ratio based sensor, the sensitivity is the rate of change of the intensity ratio with the temperature ($S = |dR/dT|$). However, in order to analyze the sensing performance of various host materials, a relative sensitivity S_R is often reported, defined as [3]:

$$S_R = \frac{S}{R} = \frac{1}{R}\left|\frac{dR}{dT}\right| = \frac{E_{32}}{K_B T^2} \quad (3)$$

From this equation it would seem that larger energy gaps for the E_{32} transition confer greater sensitivities. In practice, the separation between the energy levels must allow for significant thermalization, resulting in the upper level being sufficiently populated so as to obtain a detectable transition. Moreover, the levels need to be sufficiently separated to avoid overlap of the two fluorescence wavelengths, meaning the eligible range for the energy gaps is between 200–2000 cm^{-1}.

4. Results and discussion

4.1. Absorption and luminescence spectra of Nd^{3+} doped PKBAN samples

The absorption and luminescence spectra of the 0.1 mol% Nd^3 doped PKBAN glass samples are shown in the graph in Fig. 2(b). The absorption spectrum plotted in blue in Fig. 2(b) shows three bands centered at 750 nm, 800 nm and 870 nm with their corresponding transitions from the ground state: $^4I_{9/2} \rightarrow {}^4F_{7/2}$, $^4I_{9/2} \rightarrow {}^4F_{5/2}$ and $^4I_{9/2} \rightarrow {}^4F_{3/2}$. The energy gap between the $^4F_{5/2}$ and $^4F_{3/2}$ was determined by the distance between the centroids of the last two absorption transition bands, yielding a value of 908 cm^{-1}.

In Fig. 2(b), the luminescence resulting from laser excitation at 532 nm on the PKBAN01 sample at 310 K is plotted with a solid line, while that measured at 693 K is shown in the spectrum with a dashed black line. The mechanisms that give place to this luminescence can be followed with the aid of the energy diagram in Fig. 2(a). The pump at 532 nm excites the Nd^{3+} ions from the ground state $^4I_{9/2}$ to the $^4G_{7/2}$ levels, as represented with a green up arrow in the diagram. As a consequence of the small energy gaps between the adjacent lower levels, there are successive non- radiative de-excitations to the $^4F_{3/2}$ level, depicted with a dashed down arrow. The energy distance between the $^4F_{3/2}$ level and the next lower $^4I_{15/2}$ level is large enough to ensure that non-radiative de-excitations do not occur. Instead, radiative transitions predominate, like the relaxation to the ground state $^4F_{3/2} \rightarrow {}^4I_{9/2}$ associated with the intense emission band centered at 880 nm, shown on the diagram with a solid down arrow. Additionally, at 693 K the emission spectrum shows a strong emission band related to the $^4F_{5/2} \rightarrow {}^4I_{9/2}$ transition centered at 810 nm. This band exists at this temperature because an induced thermal redistribution of the $^4F_{3/2}$ population increments the population of $^4F_{5/2}$ and triggers the transition of the $^4F_{5/2}$ level to the ground state. Moreover, the next higher level $^4F_{7/2}$ can also be populated through thermalization from the $^4F_{5/2}$ and a weaker band associated with the $^4F_{7/2} \rightarrow {}^4I_{9/2}$ transition is evident in the spectrum at 740 nm. Thermal induced redistributions are depicted by curved red arrows in Fig. 2(a).

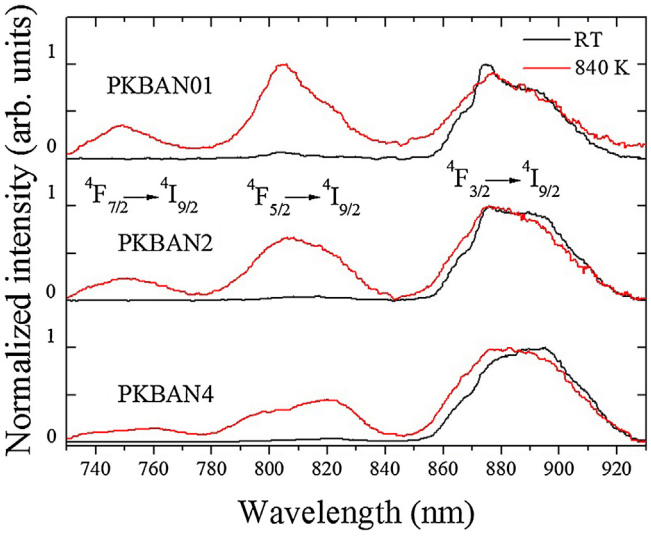

Fig. 3. Normalized spectra of PKBAN01, PKBAN2 and PKBAN4 doped glasses measured at two different temperatures: 300 K (black lines) and at 840 K (red lines). (For interpretation of the references to colour in this figure legend, the reader is referred to the web version of this article.).

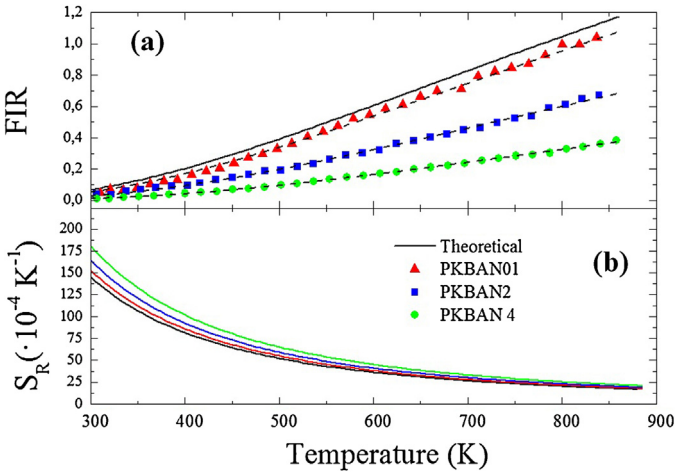

Fig. 4. (a) >Experimental fluorescence intensity ratio obtained from the $^4F_{5/2} \rightarrow {}^4I_{9/2}$ and $^4F_{3/2} \rightarrow {}^4I_{9/2}$ transitions versus temperature for the PKBAN glasses doped with 0.1, 2 and 4 mol % of Nd^{3+}. The theoretical FIR (black solid line) was calculated in the framework of the Judd–Ofelt theory (see Eq, (2)). Dashed lines are the corresponding fittings to Eq (1). (b) Relative Sensitivity of the PKBAN samples and theoretical relative sensitivity calculated from Eq (3).

Note the overlap shown in Fig. 2(b) that exists between the luminescence and absorption bands related to the same transitions. It can be also observed that the main absorption response lies in the bluer region of the emission bands associated with the $^4F_{5/2} \rightarrow {}^4I_{9/2}$ and $^4F_{3/2} \rightarrow {}^4I_{9/2}$ transition, while the absorption completely covers the $^4F_{7/2} \rightarrow {}^4I_{9/2}$ transition band. These facts may be indicative of the potential relevance of the absorption by the material of its own emission, an occurrence that is expected to gain importance as the concentration of Nd^{3+} increases.

4.2. Thermal spectrum response

Fig. 3 shows the emission spectra obtained at room temperature and at 840 K for all the samples. Notice how at high temperatures the thermalized emission bands coming from the $^4F_{5/2}$ and $^4F_{7/2}$ levels are clearly discernable. However, the ratio of intensities between the bands at 810 nm and 880 nm is different for all the samples. As will be shown later, radiative transfer processes, which depend on the concentration of the samples, can explain these differences.

Fig. 4(a) shows the dependence of the fluorescence intensity ratio on each sample's temperature in the measured range of 300–850 K. The data fitted to Eq. (1) are also plotted with the parameters given in Table 1. We see that these fittings properly reproduce the experimental data. Also, the theoretical dependence given in Eq. (2) is included in this figure. The varying behavior of the FIR response among the different samples with different concentrations is clearly evident. The dependence obtained for PKBAN01 is close to the theoretical value, with slightly lower intensity ratios. Increasing the concentration favors some kind of interaction between Nd^{3+} centers that affects the emissions associated with the transitions $^4F_{5/2} \rightarrow {}^4I_{9/2}$ and $^4F_{3/2} \rightarrow {}^4I_{9/2}$ and produces changes in the FIR dependence.

Fig. 4(b) shows the relative sensitivity values for the different doped samples in the temperature range considered. The dependence of S_R in all the samples shows a decrease when the temperature increases. Also, based on the energy gap values that resulted from the fittings of the FIR temperature responses (see Table 1), we can see that increasing the content of Nd^{3+} gives rise to greater relative sensitivity values, even greater than those obtained in the matrices reported in Refs. [6,10]. This result suggests that more sensitive results are obtained from the phosphate glass doped with 4 mol% of Nd^{3+}. Nevertheless, the results shown in Fig. 4(a)–(b) indicate that there is a discrepancy between the theoretical and the experimental results that is more noticeable when the doping concentration increases. This reveals that certain factors become more important as the Nd^{3+} doping concentration is increased, factors that are not included in the Boltzmann model. A detailed analysis is needed in order to determine how well the sensor performs in these systems.

4.3. Energy transfer processes

There are two main processes that could produce a decrease in the population of an emitting level: multiphonon relaxation and energy transfer. In multiphonon relaxation, its rate decreases with an increase of the energy gap of the emitting level with respect to its lower level. But due to the gap for the $^4F_{3/2}$ emitting level and the energy phonons in phosphate glasses, this rate can be considered negligible [15]. As for the energy transfer processes, Ref. [14] states that there is a slight chance for non-radiative transfer processes to OH^- ions, which act as traps for the energy. Moreover, the cross-relaxation processes between pairs of Nd^{3+} ions dominated by dipole-dipole interaction, which is favored when the concentration increases, could also be relevant. However, even though these effects imply a loss on the radiative decays, they do not change the band shapes, as was observed in the experimental spectra that result as a consequence of the different FIR values obtained for the doping concentrations (see Fig. 4(a)). However, radiative transfer processes between Nd^{3+} ions can affect the shape of the emission bands. These processes are due to the reabsorption of the emitted radiation by the Nd^{3+} ions. As can be seen in Fig. 2, this process could probably be due to the overlap between the emission and absorption bands. Therefore, in order to analyze these radiative transfer processes, we used the set-up described in the experimental section to obtain the emission spectra as a function of the emission path and of the Nd^{3+} concentration.

Fig. 5(a) shows the spectra of each sample corresponding to the luminescence collected at the edge and 25 mm from the edge (referred to as "inner" in the sample). The bands in each spectrum centered at 810 nm were multiplied by a factor 2 for the purpose of highlighting in the graph the differences between the surface and the luminescence collected through the thickness at this

Table 1
Data obtained in this work and in other Nd^{3+} doped samples reported in the literature. In this table shown the parameters for the FIR equation given by the Boltzmann theory as well as the absorption coefficients obtained from the absorption spectra (α_A) and from the Lambert–Beer equation fittings of the reabsorption measurements (α).

Sample	$R = B\exp(-E_{32}/K_BT)$		Temperature range (K)	S_R (K^{-1}) at 300 K	$I(x) = I_0 \times e^{-\alpha x}$		Ref.
	B	E_{32} (cm^{-1})			α(cm^{-1}) at 810 nm	α_A (cm^{-1})at 810 nm	
Theoretical	5.36	908	300–850	0.015	–	–	This work
PKBAN01	5.34	957	300–850	0.015	0.7	0.42	This work
PKBAN2	3.83	1029	300–850	0.017	9.9	9.33	This work
PKBAN4	2.50	1133	300–850	0.018	17.3	18.67	This work
SBN	4.4	953.1	300–700	0.015	–	–	[10]
Silica fiber	~2.9	1000	223–775	0.016	–	–	[6]

wavelength. In order to be able to compare the relative intensities of the bands centered at 810 nm, all the spectra were normalized to the intensity value of the sub-band centered at 905 nm. At this wavelength the absorption processes can be neglected (see Fig. 2 (b)). An arrow in the Fig. 5(a) depicts the normalized value for each sample. In general terms, for the entire range of wavelengths in the spectra, there are more differences between the inner and surface spectra when the concentration of the sample increases. The differences between the inner and surface spectra in the 0.1 mol% doped Nd^{3+} sample are small with respect to the PKBAN2 and PKBAN4 Nd^{3+} doped samples. These results are in agreement with the fact that reabsorption effects on the spectra are more pronounced when the concentration increases.

More specifically, the decrease in the $^4F_{5/2} \rightarrow {}^4I_{9/2}$ and the $^4F_{3/2} \rightarrow {}^4I_{9/2}$ emission bands can be explained by the overlapping with the respective absorption bands, as shown in Fig. 2. This further indicates that the emission from the directly excited Nd^{3+} ions interacts with other centers by means of radiative reabsorption, a critical component being the increment in the number of doping ions in the optical emission path.

It is worth noting that in the two most concentrated samples the spectra detected at their surface show profiles similar to that for the sample doped at 0.1 mol%. This is because on the surface of the most doped samples, the emission from excited Nd^{3+} ions does not pass regions with optically active ions that could reabsorb it as it travels towards the detection system.

A detailed analysis of the dependence of the intensity obtained at 810 nm, normalized as mentioned above, on the increasing path length through the sample is shown for each sample in Fig. 5(b), which was obtained using the experimental set-up shown in Fig. 1(b). The experimental data were fitted to the known Lambert Beer Law, which relates how fast light intensity decays in a material by means of its absorption coefficient at this wavelength as follows:

$$I(x) = I_0 \times e^{-\alpha x} \quad (4)$$

where I_0 is the measured emission intensity at the edge of the sample and α is the absorption coefficient. As can be seen in Fig. 5(b), the most concentrated samples result in the largest drops in emission intensity. A comparison of the absorption coefficients obtained from the fittings, α, with their values obtained from absorption spectra (α_A) is shown in Table 1. Note the relatively good concordance between both absorption coefficients, with more discrepancies for the sample with the lowest concentration due to the small effect of the reabsorption in this sample. This result leads us to conclude that the reabsorption of the emission from the directly excited ions due to other Nd^{3+} centers is the main cause behind the changes in the emission spectra profile, and therefore in the differences in the FIR response between the differently doped Nd^{3+} PKBAN samples.

From an applied point of view, we may conclude that the FIR technique for measuring the temperature of luminescence bulk samples can exhibit ambiguity if the excitation and detection emission regions do not coincide. This drawback is less relevant in lightly doped samples, as demonstrated in the results reported for PKBAN01. This fact implies a need to compromise between the higher intensity emissions than can be obtained in most doped samples and the reliability of the temperature determination. However, it would be beneficial, when implementing an optical sensor design that takes into account the low power excitation constraint, to be able to detect luminescence easily, and thus to have a high doping content. In this sense it could be interesting to use point

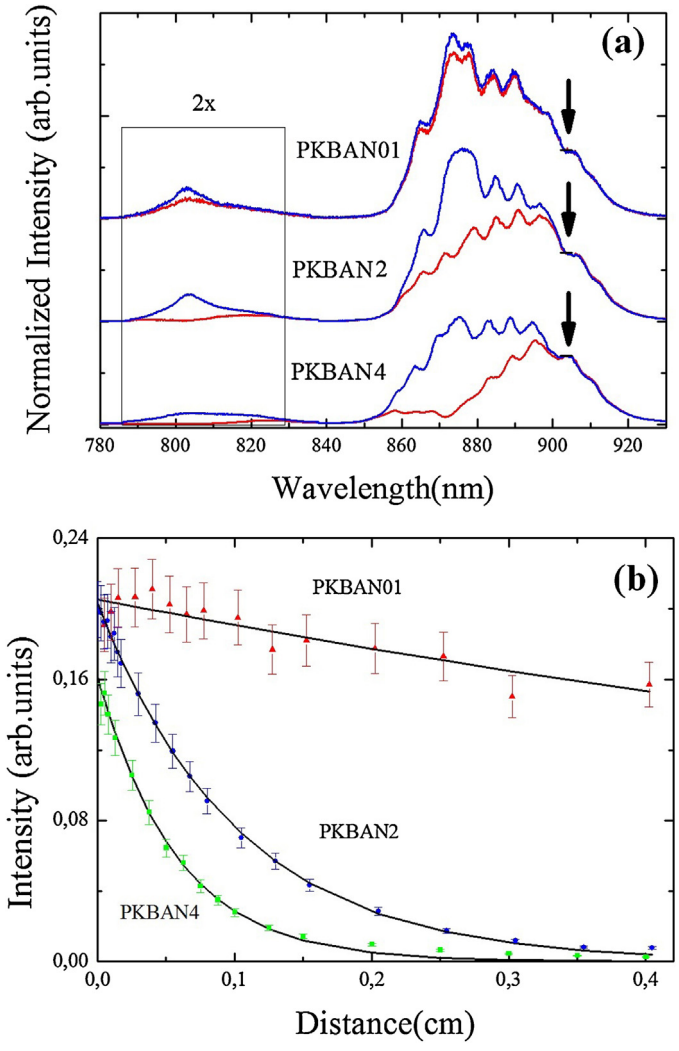

Fig. 5. (a) Normalized spectra collected exciting on the surface (blue lines) and in the inner (red lines) of the samples. (b) >Intensity obtained at 810 nm as a function of the distance between the excitation zone to the border of the sample (dots) and fitting to a Lambert–Beer dependence (solid lines). (For interpretation of the references to colour in this figure legend, the reader is referred to the web version of this article.).

sources for FIR temperature determination in order to limit the radiative transfer processes that would lead to spurious temperature determinations. Such point sources for thermal sensing are the object of current research and span everything from glass microspheres [4] to a sort of RE^{3+} doped nanoparticles in solution [23].

5. Conclusions

The luminescence of Nd^{3+} doped phosphate glasses was investigated for their application as Fluorescence Intensity Ratio based sensors. After pumping at 532 nm, the PKBAN doped Nd^{3+} show a luminescence spectrum due to transitions from the thermally coupled levels, $^4F_{3/2}$ and $^4F_{5/2}$, that exhibit a band shape that is dependent on temperature. By employing a set-up with aligned excitation and detection devices, the band shapes were also found to be dependent on the Nd^{3+} concentration. A specific optical set-up was used in order to analyze the radiative transfer processes among Nd^{3+} ions. Considering the importance of the influence of radiative transfer on the shape of the spectral bands in the samples we concluded that the PKBAN 0.1 mol% Nd^{3+} doped glass, which is less prone to radiative transfer, shows good prospects for a reliable thermal sensing. Phosphate glasses with a higher content of Nd^{3+} optically active ions also shows potential as a temperature sensor, but the reabsorption processes must first be reduced by employing small volumes, such as through the use of glass microspheres or colloidal nanoparticles.

Acknowledgements

The authors thank Spain's Ministry of Economy and Competition (MINECO) and its National Materials Program (MAT2010-21270-C04-02/-03/-04) and the Fundamental Research Program (FIS2012-38244-C02-01), the Consolider-Ingenio 2010 Program (MALTA CSD2007-0045, www.malta-consolider.com), the EU-FEDER for its financial support and the FSE and ACIISI of the Government of the Canary Islands for project ID20100152. C. Pérez-Rodríguez and L.L. Martín wish to acknowledge the ACIISSI and FSE for their thesis grants (TESIS 20100089 and Ref. TESIS2009022). S.F. León-Luis wishes to thank the MICINN for the FPI grant (BES-2008-003353). We also thank the Governments of Spain and India for the awarding of a project as part of the Indo–Spanish Joint Programme of Cooperation in Science and Technology (PRI-PIBIN-2011-1153/DST-INT-Spain-P-38-11).

Appendix A. Supplementary data

Supplementary material related to this article can be found, in the online version, at http://dx.doi.org/10.1016/j.snb.2014.01.037.

References

[1] D. Jaque, F. Vetrone, Luminescence nanothermometry, Nanoscale 4 (2012) 4301–4326.
[2] C.D.S. Brites, P.P. Lima, N.J.O. Silva, A. Millán, V.S. Amaral, F. Palacio, L.D. Carlos, Thermometry at the nanoscale, Nanoscale 4 (2012) 4799–4829.
[3] S.A. Wade, S.F. Collins, G.W. Baxter, Fluorescence intensity ratio technique for optical fiber point temperature sensing, J. Appl. Phys. 94 (2003) 4743–4756.
[4] L.L. Martín, C. Pérez-Rodríguez, P. Haro-González, I.R. Martín, Whispering gallery modes in a glass microsphere as a function of temperature, Opt. Express 19 (2011) 25792–25798.
[5] Z.P. Cai, H.Y. Xu, Point temperature sensor based on green upconversion emission in an Er:ZBLALiP microsphere, Sens. Actuators A 108 (2003) 187–192.
[6] S.A. Wade, Temperature Measurent Using Rare Earth Doped Fibre Fluorescence (Ph.D. Thesis), Victoria University, Melbourne, Australia, 1999.
[7] W.H. Fonger, C.W. Struck, Eu_5 $^{+3}$ D Resonance quenching to the charge transfer states in Y_2O_2S, La_2O_2S, and LaOCI, J. Chem. Phys. 52 (1970) 6364–6366.
[8] S.W. Allison, G.T. Gillies, A.J. Rondinone, M.R. Cates, Nanoscale thermometry via the fluorescence of YAG:Ce phosphor particles: measurements from 7 to 77 °C, Nanotecnology 14 (2003) 859–863.
[9] V.K. Rai, Temperature sensors and optical sensors, Appl. Phys. B 88 (2007) 297–303.
[10] P. Haro-González, I.R. Martín, L.L. Martín, S.F. León-Luis, C. Pérez-Rodríguez, V. Lavín, Characterization of Er^{3+} and Nd^{3+} doped strontium barium niobate glass ceramic as temperature sensors, Opt. Mater. 33 (2011) 742–745.
[11] Y. Dwivedi, S.B. Rai, Temperature-sensing behavior of Eu: BaB_4O_7 nanocrystals, Sens Actuators A Phys. 163 (2010) 37–41.
[12] D.J. Bizzak, M.K. Chyu, Use of a laser-induced fluorescence thermal imaging system for local jet impingement heat transfer measurement, Int. J.Heat Mass Transf. 38 (1995) 267–274.
[13] A.L. Heyes, S. Seefeldt, J.P. Feist, Two-colour phosphor thermometry for surface temperature measurement, Opt. Laser Technol. 38 (2006) 257–265.
[14] R. Balakrishnaiah, P. Babu, C.K. Jayasankar, A.S. Joshi, A. Speghini, M. Bettinelli, Optical and luminescence properties of Nd $^{3+}$ ions in K–Ba–Al-phosphate and fluorophosphate glasses, J. Phys. Condens. Matter 18 (2006) 165–179.
[15] F. Rivera-López, P. Babu, C. Basavapoornima, C.K. Jayasankar, V. Lavín, Efficient $Nd^{3+} \rightarrow Yb^{3+}$ energy transfer processes in high phonon energy phosphate glasses for 1.0 μm Yb^{3+} laser, J. Appl. Phys. 109 (2011) 123514–123610.
[16] E. Mura, J. Lousteau, D. Milanese, S. Abrate, V.M. Sglavo, Phosphate glasses for optical fibers: synthesis, characterization and mechanical properties, J. Non-Cryst. Solids 362 (2013) 147–151.
[17] T. Akamatsu, Continuous fabrication of a phosphate glass fiber, J. Lightw. Tecnhnol. 4 (1983) 580–584.
[18] E. Maurice, G. Monnom, B. Dussadier, A. Saissy, D.B. Ostrowsky, G.W. Baxter, Erbium-doped silica fibers for intrinsic fiber-optic temperature sensors, Appl. Opt. 34 (1995) 8019–8025.
[19] D.N. Messias, M.V.D. Vermelho, A.S. Gouveia-Neto, J.S. Aitchison, All optical integrated upconversion fluorescence-based point temperature sensing system using Er^{3+}- doped silica-on-silicon waveguides, Rev. Sci. Instrum. 73 (2002) 476–479.
[20] B. Dong, Z.Q. Feng, J.F. Zu, L. Bai, Strong visible up-conversion emissions and thermometric applications of Er^{3+}-Yb^{3+} codoped Al_2O_3 prepared by the sol–gel method, J. Sol–Gel Sci. Technol. 48 (2008) 303–307.
[21] Y. Shen, X. Wang, H. He, Y. Lin, C.-W. Nan, Temperature sensing with fluorescence intensity ratio technique in epoxy-based nanocomposite filled with Er^{3+}-doped 7YSZ, Compos. Sci. Technol. 72 (2012) 1008–1011.
[22] F. Sidiroglou, S.A. Wade, N.M. Dragomir, G.W. Baxter, S.F. Collins, Effects of high-temperature heat treatment on Nd^{3+}-doped optical fibers for use in fluorescence intensity ratio based temperature sensing, Rev. Sci. Instrum. 74 (2003) 3524–3530.
[23] U. Rocha, C.J. da Silva, W. Ferreira Silva, I. Guedes, A. Benayas, L. Martínez Maestro, M. Acosta Elias, E. Bovero, F.C.J.M. van Veggel, J.A. García Solé, D. Jaque, Subtissue thermal sensing based on neodymiun-doped LaF_3 nanoparticles, ACS Nano 7 (2013) 1188–1199.
[24] S.F. León-Luis, U.R. Rodríguez-Mendoza, P. Haro-González, I.R. Martín, V. Lavín, Role of the host matrix on the thermal sensitivity of Er^{3+} luminescence in optical temperature sensors, Sens. Actuators B 174 (2012) 176–186.
[25] A. Stoita, T. Vautey, B. Jacquier, S. Guy, Impact of the radiation trapping on lifetime measurement of Er^{3+} doped glasses, J. Lumin. 130 (2010) 1119–1123.
[26] D. Li, Y. Wang, X. Zhang, K. Yang, L. Liu, Y. Song, Optical temperature sensor through infrared excited blue upconversion emission in Tm^{3+}/Yb^{3+} codoped Y_2O_3, Opt. Commun. 285 (2012) 1925–1928.
[27] W. Xu, X. Gao, L. Zheng, Z. Zhang, W. Cao, An optical temperature sensor based on the upconversion luminescence from Tm^{3+}/Yb^{3+} codoped oxyfluoride glass ceramic, Sens. Actuators B 173 (2012) 250–253.

Biographies

Carla Pérez-Rodríguez received the M.Sc. degree in 2010 at the University of La Laguna (Spain) where she is currently a Ph.D. student. During her Ph.D. has worked in the fields of spectroscopy of fluorophores and rare earth doped glasses, spherical micro-resonators made of rare earth doped glasses for sensing applications and lately, in the lensing properties of microspheres.

Leopoldo Luis Martín received a Ph.D. at the University of La Laguna (Spain) in 2013. During his Ph.D. has worked in the fields of spectroscopy of rare earth doped glasses, glass micro modification by laser techniques and lately, in spherical micro-resonators made of rare earth doped glasses for sensing applications. Currently he is a postdoctoral researcher at Technion University (Israel) in the professor Tal Carmon' laboratory.

Sergio F. León Luis received the M.Sc. degree in 2008 at the University of La Laguna (Spain), and is a candidate for a Ph.D. degree. He joined the Laser Spectroscopy and High Pressure group and has worked on optical materials for the last 4 years. He also belongs to The MALTA Project (www.malta-consolider.com) that includes more than 70 scientists from 12 Spanish research groups dedicated to the study of diverse high pressure phenomena under a variety of different perspectives. His research interests cover the optical spectroscopy of rare earth ions at ambient and extreme conditions of pressure and temperature.

Inocencio R. Martín is Associate Professor at the Department of Fundamental and Experimental Physics at the University of La Laguna, Spain. He received a Ph.D. in 1996 from the University of La Laguna. He is a member of the Laser Spectroscopy and High Pressure group and the MALTA Project and his research interests cover the optical characterization of glasses, crystals and nanocrystalline glass-ceramics

doped with optically active ions. He has over 110 publications in peer reviewed journals and conference proceedings. Currently he is involved in optical characterization of microspheres doped with rare-earth ions and their applications in sensors.

K. Kiran Kumar received his Master degree in Physics in 1999 from Sri Venkateswara University, Tirupati, India and currently he is working for his Ph.D. degree. He joined in the Photonics group in the Department of Physics and working on the "Solid state spectroscopy of rare earth elements" for the last five years.

C. K. Jayasankar is a Professor at the Department of Physics, Sri Venkateswara University, Tirupati, India. He received his Ph.D. degree in 1984 from Sri Venkateswara University, Tirupati. He is having 24 years of teaching experience for students of Master of Science in Physics besides 34 years of research experience in the field of Solid State Spectroscopy and development of luminescent materials. He has over 165 publications in internationally reputed journals and conference proceedings. Presently he is involved in optical characterization of lanthanide doped glasses, glass-ceramics and nanocrystals for photonic applications.